Available online at www.sciencedirect.com
ScienceDirect
Ceramics International 38S (2012) S135–S139
CERAMICS INTERNATIONAL
www.elsevier.com/locate/ceramint

Al_2O_3–cyanate ester hybrid thick films through aerosol deposition and resin infiltration

Hyung-Jun Kim [a], Yoon-Hyun Kim [a], Young-Hoon Yun [b], Song-Min Nam [a,*]

[a] Department of Electronic Materials Engineering, Kwangwoon University, 447-1, Wolgye-dong, Nowon-gu, Seoul 139-701, Republic of Korea
[b] Department of Hydrogen & Fuel Cell Technology, Dongshin University, Jeonnam 520-714, Republic of Korea

Available online 30 April 2011

Abstract

Al_2O_3–cyanate ester hybrid thick films had high Al_2O_3 contents over 75 vol.% were fabricated as 3D integrated substrates. The Al_2O_3–cyanate ester hybrid thick films were completed by resin infiltration of the cyanate ester into the porous Al_2O_3 thick films deposited by aerosol deposition (AD). Al_2O_3 particles were packed as high-density layers in the porous Al_2O_3 thick films by controlling the carrier gas flow rate using AD at room temperature. As dielectric substrate materials, the Al_2O_3–cyanate ester hybrid thick films had dielectric constant of 7.6 and quality (Q) factor of 390, and both were nearly independent of the measuring frequency.

Keywords: A. Films; B. Composites; D. Al_2O_3; E. Substrates

1. Introduction

With the modern needs for wireless communication and portable devices, electronic devices continue to gain functionality at higher operating speeds with enhanced miniaturization as a result of the increasing integration of electronic components. Therefore, integration technologies have been developed for electronic components to increase packaging density within a limited area. Therefore, three-dimensional (3D) integrations such as systems on a package, with higher packaging densities achieved using embedded passive technology, were proposed to overcome the limitation of surface mount technology [1,2].

For application as integrated substrates in 3D integrations, co-fired ceramics and polymers have been researched as thick film processes [3]. However, co-fired ceramic substrates still require high-temperature processing at approximately 850 °C, which limits the use of active devices and chip components due to interdiffusion and reactions, and the resulting ceramic brittleness can also lead to serious problems during the 3D lamination process [4]. Moreover, polymer substrates require improved thermal conductivity and dissipation factor, and the mismatch of the different components' coefficients of thermal expansion is another outstanding issue. Therefore, high performance hybrid substrates consisting of a polymer resin with ceramic fillers have been researched to overcome these material limits, although cost effective processes have not yet been developed [5].

In this study, a novel concept was used to fabricate ceramic–polymer hybrid thick films by using aerosol deposition (AD) and resin infiltration. At first, the AD process was applied for the fabrication of dense ceramic thick films without pores at room temperature through solidification of nano-crystallites by strong impact of ceramic starting powder [6]. In comparison, the deposited ceramic films formed a porous microstructure similar to that of a pressed compact if nano-sized ceramic particles below 100 nm were used as the starting powder due to their insufficient impact energy. Based on this phenomenon, we attempted to fabricate porous ceramic thick films with a structure featuring the high-density packing of ceramic nanoparticles by controlling the carrier gas flow rate. Moreover, these ceramic–polymer hybrid thick films were fabricated for high performance integrated substrates by infiltrating polymer resin into the porous thick films.

2. Experimental

Fig. 1 shows the proposed method for the fabrication of ceramic–polymer hybrid thick films using AD and resin

* Corresponding author. Tel.: +82 2 9405764; fax: +82 2 9425764.
E-mail address: smnam@kw.ac.kr (S.-M. Nam).

0272-8842/$36.00
doi:10.1016/j.ceramint.2011.04.067

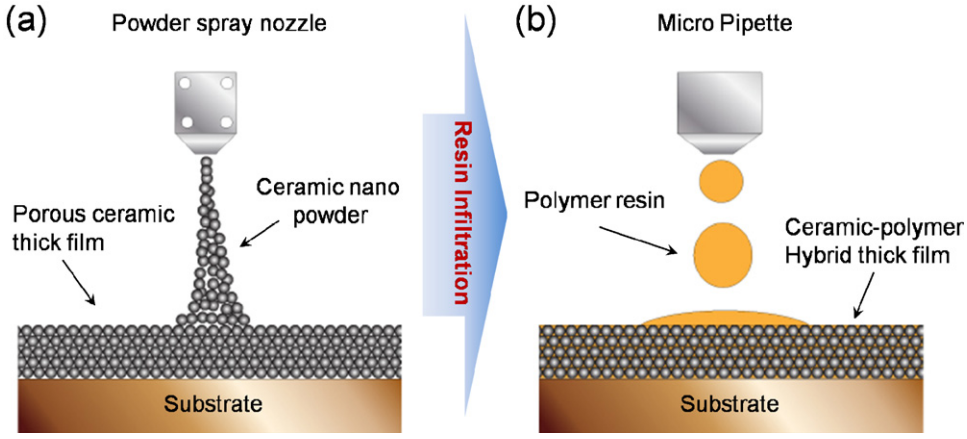

Fig. 1. Schematics of the fabrication of (a) porous ceramic thick films by AD process and (b) ceramic–polymer hybrid thick film by resin infiltration.

infiltration. The first step is the fabrication of porous ceramic layers by high-density packing of ceramic particles by using the AD process, and the second is the resin infiltration into the pores in the porous ceramic layers. As the ceramic starting powder, spherical Al_2O_3 nano-powder 'Denka UFP30′ with an average diameter of 200 nm, which included many small particles below 100 nm, was prepared.

The Al_2O_3 starting powder was aerosolized in an aerosol chamber by means of a vibration and mixing system with He carrier gas. The Al_2O_3 powders were transported by the carrier gas and accelerated through a nozzle. The accelerated Al_2O_3 powders were ejected and deposited onto Cu substrates by the high-speed gas flow. To improve the surface roughness of the deposited films and packing density, we confirmed the effect on the variation of the surface morphologies of varying the carrier gas flow rate from 1 standard liter per minute (slm) to 10 slm. The microstructure and crystallinity of the deposited Al_2O_3 films were analyzed by scanning electron microscope (SEM) 'Hitachi S-4700′ and X-ray diffraction (XRD) 'PANalytical X' Pert PRO', respectively.

As a polymer resin, a thermoset cyanate ester resin was prepared as a solution of 2 wt.% with dimethyl formamide. The cyanate ester resin was spread on the porous Al_2O_3 thick films deposited by AD using a spin coater for uniform infiltration. The Al_2O_3–cyanate ester hybrid thick films were heated to 280 °C for 5 h in an electric tube furnace in a N_2 atmosphere to cure the cyanate ester. The dielectric properties were measured by an impedance analyzer (Agilent 4294A). The Al_2O_3 contents in the hybrid thick films were calculated by Hashin–Shtrikman bounds using the measured dielectric constant [7]. The following equation shows the d-dimensional Hashin–Shtrikman bounds on the relative permittivity of composites for two-phase isotropic media in which $\varepsilon_2 \geq \varepsilon_1$ are

$$\varepsilon_L \leq \varepsilon_C \leq \varepsilon_U, \tag{1}$$

$$\varepsilon_U = \langle \varepsilon \rangle - \frac{V_1 V_2 (\varepsilon_2 - \varepsilon_1)^2}{\langle \tilde{\varepsilon} \rangle + (d-1)\varepsilon_1}, \tag{2}$$

$$\varepsilon_L = \langle \varepsilon \rangle - \frac{V_1 V_2 (\varepsilon_2 - \varepsilon_1)^2}{\langle \tilde{\varepsilon} \rangle + (d-1)\varepsilon_2}, \tag{3}$$

$$\langle \varepsilon \rangle = \varepsilon_1 V_1 + \varepsilon_2 V_2, \tag{4}$$

$$\langle \tilde{\varepsilon} \rangle = \varepsilon_1 V_2 + \varepsilon_2 V_1, \tag{5}$$

where ε_U and ε_L are the top and bottom limits of the possible relative permittivity of composites (ε_C), respectively, ε_1 and ε_2 are the relative permittivities of the materials, V_1 and V_2 are the volume fractions of materials, and the dimensional constant d is 3.

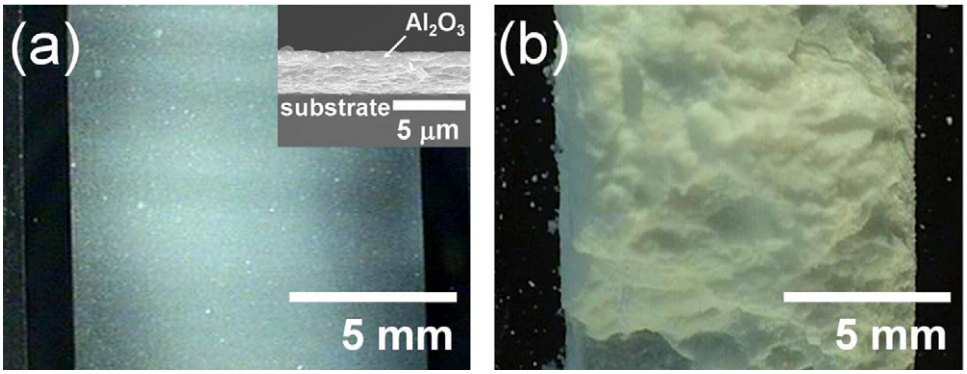

Fig. 2. Photographs of (a) the aerosol-deposited dense Al_2O_3 thick films on Si wafer, with a cross-sectional SEM image in the inset, and (b) the aerosol-deposited Al_2O_3 pressed compact on Si wafer using Al_2O_3 nano starting powder (<100 nm).

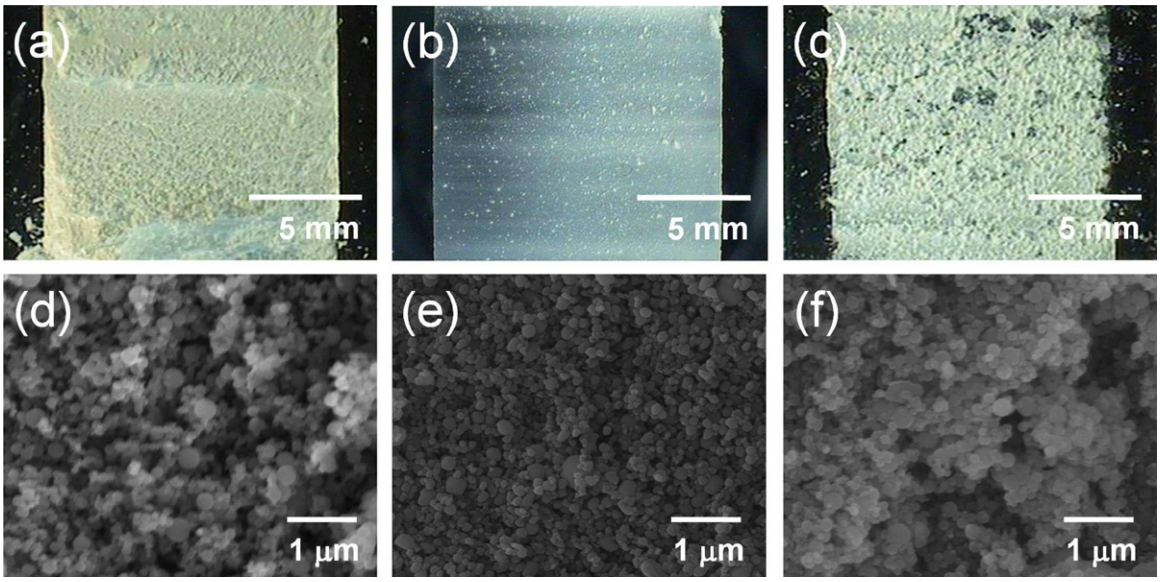

Fig. 3. Variation of surface morphology and packing density of the deposited films as a function of the carrier gas flow: (a) below 2.5 slm, (b) 3 slm, and (c) 5 slm. (d)–(f) Their surface SEM images.

3. Results and discussion

In general, aerosol deposited ceramic thick films such as Al_2O_3 thick films using submicron fine particles as the starting powders exhibited dense structures without pores, as shown in Fig. 2(a). In comparison, porous structures such as the pressed compact were deposited using nano-sized ceramic starting particles below 100 nm with extremely high deposition rates over 100 μm/min, as shown in Fig. 2(b).

The results revealed that the density of the deposited films was affected by the carrier gas flow rate, as shown in Fig. 4. At low flow rates below 2.5 slm, the deposited Al_2O_3 films exhibited rough surface morphology with low packing density, as shown in Fig. 3(a). In comparison, the packing density was noticeably improved by increasing the carrier gas flow rate over the critical value, and the surface morphology also became flat as shown in Fig. 3(b). However, the deposited Al_2O_3 films were etched by an excessively strong carrier gas flow rate over 5 slm due to the increased impact energy, as shown in Fig. 3(c).

In general, aerosol-deposited, ceramic thick films such as Al_2O_3 thick films show a small crystallite size below 20 nm, despite the several hundred nanometer-sized starting powders, because of the particle crushing that occurs when they collide with the substrates. Therefore, XRD patterns of the deposited ceramic thick films show peak broadening caused by the reduced crystallite size compared to that of the starting powder [6]. In comparison, the XRD patterns of the deposited porous Al_2O_3 thick films did not show such peak broadening, as shown in Fig. 4, because the porous Al_2O_3 thick films were deposited without any crushing of the starting powders. The detailed mechanism of the adhesion and packing of ceramic particles in the porous ceramic thick films has not yet been fully clarified. Clearly, however, the mechanism of the aerosol-deposited, porous ceramic thick films differs from that of dense ceramic thick films fabricated by the conventional AD process based on

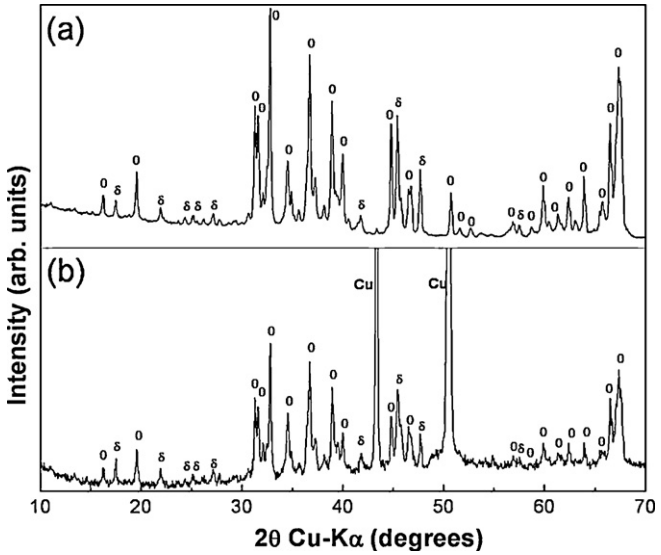

Fig. 4. XRD analysis of (a) the Al_2O_3 starting powder and (b) the porous Al_2O_3 thick film deposited on the Cu substrate by AD process.

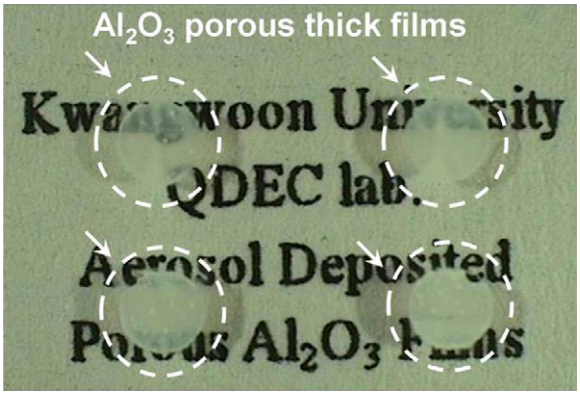

Fig. 5. Translucent porous Al_2O_3 thick films deposited by AD process with high packing density on the glass substrate.

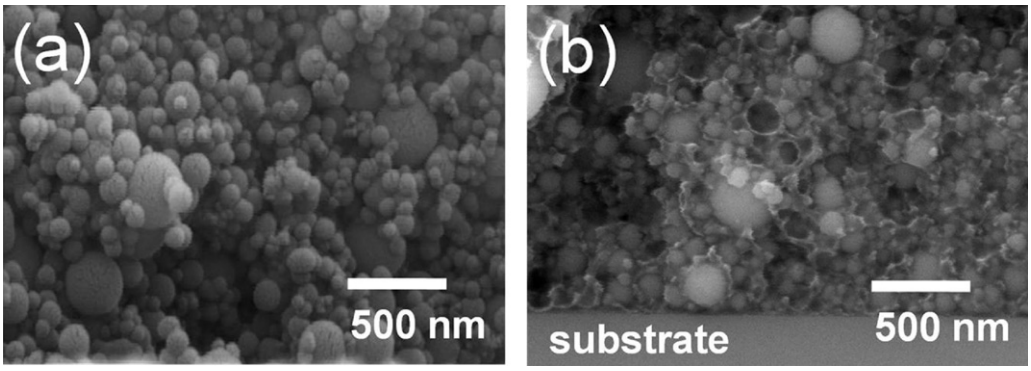

Fig. 6. Cross-sectional SEM images of (a) the porous Al_2O_3 thick film deposited by AD process and (b) the Al_2O_3–cyanate ester hybrid thick film after the resin infiltration.

the impact and solidification of submicron particles. Deposition of porous ceramic thick films does not lead to the crushing of starting particles during the deposition. These results suggest that these deposited films will be able to maintain the desired properties of the starting powders such as the crystallinity, and dielectric and mechanical properties.

Fig. 5 shows the porous Al_2O_3 thick films with high packing density deposited by AD on the glass substrate. In general, the distribution of closed pores in polycrystalline films or nano-porous films affects the decrease of transparency due to internal scattering by pores, so the deposited translucent porous films mean high packing density of nano-particles compared to the pressed compacts in Fig. 2(b) [8]. As shown in Fig. 6, we could assume that the high packing density of the Al_2O_3 particles allowed the formation of the translucent deposited porous Al_2O_3 thick films with low porosity. To examine the packing density more clearly, the microstructures of the deposited films were analyzed by SEM observations.

Fig. 6(a) shows the cross-sectional SEM image of the porous Al_2O_3 thick films on the glass substrates before the resin infiltration. The microstructures of the porous Al_2O_3 thick films showed the high packing density of the spherical Al_2O_3 nano-starting particles. To fabricate Al_2O_3 ceramic–polymer hybrid thick films, the cyanate ester polymer resin was sprayed on the porous Al_2O_3 thick films by spin coating in order to achieve uniform infiltration. As a result, the cyanate ester resin was fully infiltrated into the interface between the substrates and the Al_2O_3–cyanate ester hybrid thick films were fabricated, as shown in Fig. 6(b). The porous Al_2O_3 thick films maintained the shapes and connectivity of particles during the infiltration.

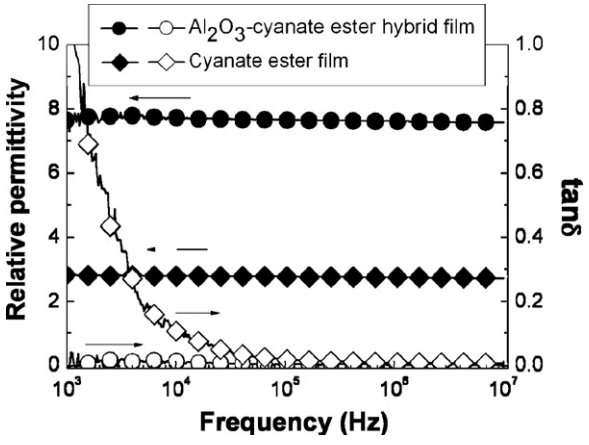

Fig. 7. Dielectric properties of the Al_2O_3–cyanate ester hybrid thick films and the cyanate ester thick films as a function of frequency.

To cure the cyanate ester, the Al_2O_3–cyanate ester hybrid thick films were heated to 280 °C for 5 h by the electric tube furnace in the N_2 atmosphere. Fig. 7 shows the dielectric properties of the Al_2O_3–cyanate ester hybrid thick films (30 μm thick) and the cyanate ester thick films (10 μm thick) fabricated by spin coating and curing. The dielectric constant and loss tangent of the cyanate ester thick films were 2.7 at 1 MHz and 0.007 (Q factor = 135) after curing at the same condition with the cyanate ester films, respectively. For the Al_2O_3–cyanate ester hybrid thick films fabricated by AD and resin infiltration, the dielectric constant was increased to 7.6, but the loss tangent was remarkably decreased to 0.0025 (Q factor = 390), due to the superior dielectric properties of the Al_2O_3 ceramic particles as fillers in the hybrid thick films.

Moreover, we confirmed the high Al_2O_3 loading in the hybrid thick films based on calculations using Hashin–Shtrikman bounds as a mixing rule of the Al_2O_3 and the cyanate ester. In the previous study, we found that the dielectric constant of composite films by AD tended to follow the top limits [9]. Using the result, the calculated Al_2O_3 contents were higher than 75 vol.% in the composite films. The closed pores occupied little volume in the hybrid thick films were not concerned, but the calculated Al_2O_3 content would be actually increased if the pores are concerned with the mixing system.

4. Conclusions

We demonstrated the porous Al_2O_3 thick films by aerosol deposition, and the porosity and surface roughness could be controlled by carrier gas flow. Also, Al_2O_3–cyanate ester hybrid thick films were fabricated by resin infiltration, and the connectivity of particles was sufficiently strong to maintain the shapes for the resin infiltration. The hybrid thick films exhibited superior dielectric properties as integrated substrates. The

Al_2O_3 contents calculated from the Hashin–Shtrikman bounds were higher than 75 vol.%.

Acknowledgements

This research was supported by a grant from the Fundamental R&D Program for Core Technology of Materials funded by the Ministry of Commerce, Knowledge and Economy, Republic of Korea. Also, this work was supported by the Grant of the Korean Ministry of Education, Science and Technology (The Regional Core Research Program/Biohousing Research Institute).

References

[1] R.R. Tummala, V.K. Madisetti, System on chip or system on package? IEEE Design & Test Computers 99 (1999) 48–56.

[2] A.S. Brown, W.A. Doolittle, N.M. Jokerst, S. Kang, S. Huang, S.W. Seo, Heterogeneous materials integration: compliant substrates to active device and materials packaging, Materials Science and Engineering B 87 (3) (2001) 317–322.

[3] The international technology roadmap for semiconductors (ITRS) 2009 Edition, Assembly and Packaging.

[4] D.P.H. Hasselman, Thermal stress resistance of engineering ceramics, Materials Science and Engineering 71 (1985) 251–264.

[5] H. Windlass, P.M. Raj, D. Balaraman, S.K. Bhattacharya, R.R. Tummala, Polymer–ceramic nanocomposite capacitors for system-on-package (SOP) applications, IEEE Transactions on Advanced Packaging 26 (1) (2003) 10–16.

[6] J. Akedo, Room temperature impact consolidation (RTIC) of fine ceramic powder by aerosol deposition method and applications to microdevices, Journal of Thermal Spray Technology 17 (2008) 181–198.

[7] S. Torquato, Random Heterogeneous Materials: Microstructure and Macroscopic Properties, Springer, 2005.

[8] S. Ma, W.Q. Quek, Q.F. Li, Y.F. Zhang, J.Y.H. Fuh, L. Lu, Sintering of translucent alumina, Journal of Materials Processing Technology 209 (2009) 4711–4715.

[9] H.J. Kim, Y.H. Kim, S.M. Nam, Calculation of Al_2O_3 contents in Al_2O_3–PTFE composite thick films fabricated by using the aerosol deposition, Journal of the Korean Physical Society 57 (4) (2010) 1086–1091.